MucosalImmunology

www.nature.com/mi

ARTICLE

Long-lived regulatory T cells generated during severe bronchiolitis in infancy influence later progression to asthma

Jason P. Lynch[1,2], Rhiannon B. Werder[1,2], Bodie F. Curren[1,2], Md. Al Amin Sikder[1,2], Ashik Ullah[1], Ismail Sebina[1], Ridwan B. Rashid[1,2], Vivian Zhang[1,2], John W. Upham[3,4], Geoff R. Hill[5], Raymond J. Steptoe[3] and Simon Phipps[1,4]

The type-2 inflammatory response that promotes asthma pathophysiology occurs in the absence of sufficient immunoregulation. Impaired regulatory T cell (Treg) function also predisposes to severe viral bronchiolitis in infancy, a major risk factor for asthma. Hence, we hypothesized that long-lived, aberrantly programmed Tregs causally link viral bronchiolitis with later asthma. Here we found that transient plasmacytoid dendritic cell (pDC) depletion during viral infection in early-life, which causes the expansion of aberrant Tregs, predisposes to allergen-induced or virus-induced asthma in later-life, and is associated with altered airway epithelial cell (AEC) responses and the expansion of impaired, long-lived Tregs. Critically, the adoptive transfer of aberrant Tregs (unlike healthy Tregs) to asthma-susceptible mice failed to prevent the development of viral-induced or allergen-induced asthma. Lack of protection was associated with increased airway epithelial cytoplasmic-HMGB1 (high-mobility group box 1), a pro-type-2 inflammatory alarmin, and granulocytic inflammation. Aberrant Tregs expressed lower levels of CD39, an ectonucleotidase that hydrolyzes extracellular ATP, a known inducer of alarmin release. Using cultured mouse AECs, we identify that healthy Tregs suppress allergen-induced HMGB1 translocation whereas this ability is markedly impaired in aberrant Tregs. Thus, defective Treg programming in infancy has durable consequences that underlie the association between bronchiolitis and subsequent asthma.

Mucosal Immunology _####################_; https://doi.org/10.1038/s41385-020-0268-8

INTRODUCTION

Asthma is a chronic inflammatory disease typically associated with a deleterious type-2 inflammatory response orchestrated by CD4+ T helper 2 (Th2) cells and type-2 innate lymphoid cells (ILC2s). Critically, this over-exuberant type-2 inflammation occurs in the absence of appropriate immunosuppression by regulatory T (Treg) cells.[1,2] In recent years, many of the cellular and molecular processes that contribute to the development of type-2 immunity have been elucidated. Most notably, superimposed on the archetypal DC-mediated clonal expansion of antigen-specific T cells, it has emerged that other innate cells (e.g., ILC2s, mast cells, and basophils) contribute to Th2 cell priming, and that all of these cell types receive signals from the activated airway epithelium.[3–5] This instruction comes in the form of "alarmins" such as high mobility group box (HMGB)1 and IL-33: cytokine-like molecules that are typically sequestered in the cell nucleus and released upon cellular stress or death. The expression of these molecules is elevated upon allergen or virus exposure and correlates with asthma severity, and both are considered therapeutic targets. In contrast, intervention strategies aimed at promoting greater immunosuppression are lagging.

Treg cells are essential for maintaining self-tolerance and immune homeostasis. Treg cell numbers are typically lower in the lung and BALF in both pediatric and adult asthma,[6–8] the Treg cell to conventional T cell ratio is lower in patients that develop a dual early and late phase response,[1] and Treg cell numbers and their suppressive capacity fall during acute exacerbations.[9,10] Diminished suppressive capacity has been ascribed to impaired production of the immunoregulatory cytokine IL-10 and lower surface expression of the ectonucleotidase CD39.[2,11] Despite these findings, there is presently a paucity of evidence to explain why asthmatics develop impaired Treg cell responses.

Severe respiratory syncytial virus (RSV) bronchiolitis in early-life is a major independent risk factor for the development of subsequent asthma,[12–14] an association that is significantly greater in children who later become sensitized to aeroallergens, conferring the greatest risk for progression to severe asthma.[15,16] Whether defects in the Treg cell compartment contributes to these associations remains unknown, however hospitalized infants with severe RSV bronchiolitis have lower frequencies of Treg cells,[17,18] and in mouse models of RSV bronchiolitis, Treg cells prevent immunopathology.[19,20] Notably, environmental exposures that lower asthma risk such as farm living, helminthic infections, or breastfeeding, are associated with elevated Treg cell numbers.[21,22] Collectively, these findings suggest that aberrant Treg cell programming is imprinted in infancy and predisposes to the inception and progression of asthma in later childhood.

We recently developed a preclinical model of viral bronchiolitis and subsequent asthma by transiently depleting pDCs during neonatal infection with PVM (pneumonia virus of mice), the murine analog of human RSV.[20] The severe bronchiolitis that develops in early-life is characterized by epithelial damage,

[1]Respiratory Immunology, QIMR Berghofer Medical Research Institute, Herston, Queensland 4006, Australia; [2]School of Biomedical Sciences, University of Queensland, Queensland 4072, Australia; [3]UQ Diamantina Institute, The University of Queensland, Queensland 4102, Australia; [4]Australian Infectious Diseases Research Centre, The University of Queensland, Queensland 4072, Australia and [5]Fred Hutchinson Cancer Research Center, Seattle, WA 1100, USA
Correspondence: Simon Phipps (Simon.Phipps@qimrberghofer.edu.au)

Received: 31 July 2019 Revised: 22 January 2020 Accepted: 26 January 2020
Published online: 17 February 2020

© Society for Mucosal Immunology 2020

pro-inflammatory cytokine production, and type-2 inflammation, is attributable to defective Treg cell expansion and function,[20] and predisposed towards subsequent asthma in later life upon secondary infection, implicating a causal relationship between bronchiolitis and later asthma. In the present study, we assessed whether severe bronchiolitis leads to long-lived alterations in mucosal immunity that predispose to later allergic sensitization and asthma, and assessed whether the functional capability of Treg cells generated during viral bronchiolitis in infancy influences this aberrant mucosal response.

RESULTS

Severe bronchiolitis in pDC$^{\Delta}$ mice predisposes toward allergen induced asthma

To determine whether severe bronchiolitis in infancy would predispose to the subsequent development of allergen-induced asthma, WT and BDCA2-DTR transgenic (hereafter referred to as pDC$^{\Delta}$) neonatal mice were treated with diphtheria toxin (to transiently deplete pDC; i.e., pDC return to steady-state levels within 10 days post infection (dpi)),[20] inoculated with PVM (10 pfu; i.n. route), then challenged with cockroach extract (CRE; 1 µg) at 42, 49, 56, and 63 dpi (Fig. 1a). In pDC$^{\Delta}$ mice, the development of severe bronchiolitis in infancy induces a pronounced granulocytic inflammation in early-life,[20] however, this phenotype did not persist into later childhood (i.e., at 66 dpi; Fig. 1b). Similar to our previous findings,[5] repeated exposure to low-dose CRE alone did not induce eosinophilic or neutrophilic inflammation in the airways (Fig. 1b). However, in the infected pDC$^{\Delta}$ mice, which develop severe viral bronchiolitis in infancy,[20] but not in the infected WT mice that experienced a mild bronchiolitis in infancy, later CRE exposure induced a marked increase in granulocytic inflammation (Fig. 1b). Eosinophils can be supported by IL-5, a maturation and survival factor, however, when sampling three days after the final low-dose CRE exposure, neither the expression of IL-5 (data not shown) nor numbers of ILC2s, ST2+ CD8+ T cells and ST2+ CD4+ T cells (i.e., potential sources of IL-5), were different between groups (Fig. 1c and Fig. S1a–e). The concentration of serum CRE-specific IgG1 (Fig. S1f) or CRE-specific IgE (undetectable) was not different either. However, similar to the granulocytic phenotype, mice that developed severe, but not mild, viral bronchiolitis in infancy and were exposed to CRE in later life presented with mucus cell metaplasia (Fig. 1d), increased airway smooth muscle (ASM) area (Fig. 1e), and greater airway hyperreactivity (Fig. 1f, g). These pathologies were absent in infected pDC$^{\Delta}$ mice that were not exposed to CRE in later-life (Fig. 1 and Fig. S1). These cardinal features of asthma were not increased in WT mice, even after exposure to both virus and CRE. Collectively, these data suggest that severe viral bronchiolitis predisposes to allergen-induced experimental asthma.

Severe bronchiolitis in pDC$^{\Delta}$ mice sensitizes to aeroallergen

We reasoned that severe bronchiolitis in infancy alters the airway response to the initial CRE exposure at 42 dpi, facilitating asthma inception. Three days after the CRE exposure (i.e., at 45 dpi; Fig. 2a), the numbers of airway eosinophils and neutrophils (Fig. 2b), ST2+ CD4+ T cells (lung and MLN; Fig. 2c, d) and ILC2s (lung and MLN; Fig. 2e, f) were all signficantly elevated in pDC$^{\Delta}$ mice, compared to WT mice, that been infected in early-life. Despite the increased number of ST2+ CD4+ T cells (putative Th2 cells) and ILC2s, this was not associated with an increase in Th2-inducing cytokine (IL-33, TSLP, and IL-25) or Th2 effector cytokine (IL-5, IL-13) levels in BALF (data not shown). As both cDC and moDCs are implicated in initiating Th2 immunity,[23] we measured these cells in the lungs and MLNs. cDCs were significantly increased in both compartments of pDC$^{\Delta}$ mice compared to WT mice (Fig. 2g and Fig. S2a), whereas moDCs and CD103 DCs were unaffected by mouse genotype (Fig. S2a, b).

We and others have identified that epithelial-derived HGMB1 contributes to allergen-induced type-2 inflammation, an effect that is partially mediated through the activation of DCs.[4,24] The nuclear-to-cytoplasmic HMGB1 translocation preceeds its extracellular release, and so is a useful measure of AEC activation. Three days after CRE, the proportion of cytoplasmic HMGB1 expressing AECs was significantly greater in pDC$^{\Delta}$ mice compared to WT mice (Fig. 2h). Intriguingly, even without CRE, the number of cytoplasmic-HMGB1+ AEC cells was significantly greater in pDC$^{\Delta}$ mice compared to WT mice that had been infected with PVM as neonates (Fig. 2h). As expected, this phenotype was also apparent at 42 dpi (Fig. 2i). These findings suggest that severe bronchiolitis in infancy leads to a long-lived alteration in the epithelium that might contribute to the onset of later asthma.

Anti-HMGB1 ablates CRE-induced granulocytic inflammation in predisposed pDC$^{\Delta}$ mice

To determine whether HMGB1 contributed to the elevated immune response observed in the pDC$^{\Delta}$ mice, we repeated the sensitiation model and treated the mice with anti-HMGB1 or an isotype-matched control at 40, 41 and 43 dpi (i.e., −2, −1, and +1 days post CRE; Fig. 3a). In the pDC$^{\Delta}$ mice, the heightened proportion of AECs expressing HMGB1 was significantly decreased following treatment with anti-HMGB1 (Fig. 3b), consistent with the auto-amplification effect of HMGB1[4]. In pDC$^{\Delta}$ mice, this decrease in cytoplasmic HMGB1+ epithelial cells was accompanied by a decrease in the number of neutrophils and eosinophils in the airways (Fig. 3c) The total cell count was also significantly decreased in the lungs, however this was not associated with a change in the numbers of ST2+ T cells or ILC2s (Fig. S2c). Lung neutrophils and eosinophils were not enumerated.

Severe viral bronchiolitis predisposes to allergic sensitization through bystander CD4+ Th2 cell activation

Severe PVM bronchiolitis increased the numbers of ST2+ CD4+ T cells in the MLN and lungs following primary CRE exposure, suggesting a predisposition to allergic sensitization. CRE-specific TCR transgenic mice are not available, so to test the hypothesis that severe viral bronchiolitis promotes CD4+ Th2 cell differentiation to a bystander antigen, we crossed OVA-specific TCR transgenic mice (OT-II) with 4C13R mice[25] to generate OVA-specific CD4+ T cells that would report for IL-4 (AmCyan) and IL-13 (dsRed). We then adoptively transferred (i.v. route) naïve T cells (CD3+ CD4+, CD44^{lo}, and CD62L^{hi}) at 42 dpi to WT and pDC$^{\Delta}$ mice that had been infected in early life (Fig. 4a), and exposed the mice to OVA and CRE (to activate the innate immune response) 2 h later. In response to OVA/CRE exposure, there was a marked and significant increase in IL-13 single-positive and IL-4/13 double-positive OT-II cells in the MLN of pDC$^{\Delta}$ but not WT mice at 47 dpi (Fig. 4b). As expected, exposure to OVA or CRE alone did not induce a difference in OT-II Th2 cell numbers between WT and pDC$^{\Delta}$ mice.

Defective Treg cells generated in early-life persist and remain impaired in later-life

In mice, pDCs confer protection from severe bronchiolitis and subsequent asthma by promoting the expansion of Nrp1+ Treg cells during PVM infection.[20] In the absence of pDC, Treg cell CD39 expression and IL-10 production is low, suggesting that the cells are functionally impaired.[20] To address whether the progression to either virus-induced or allergen-induced asthma in pDC$^{\Delta}$ mice is underpinned by a failure of long-lived Treg cells to control airway inflammation in later-life, we first quantified the number of Nrp1+ Treg cells at the time of reinfection (42 dpi), and at 1, 3, and 7 days (43, 45, and 49 dpi) after PVM challenge (Fig. 5a). At 42 dpi, Treg cell numbers in the lung and MLN did not differ between WT and pDC$^{\Delta}$ mice; however, 3 days after secondary infection, Nrp1+ Treg cells were significantly elevated in both compartments (Fig. 5b) in

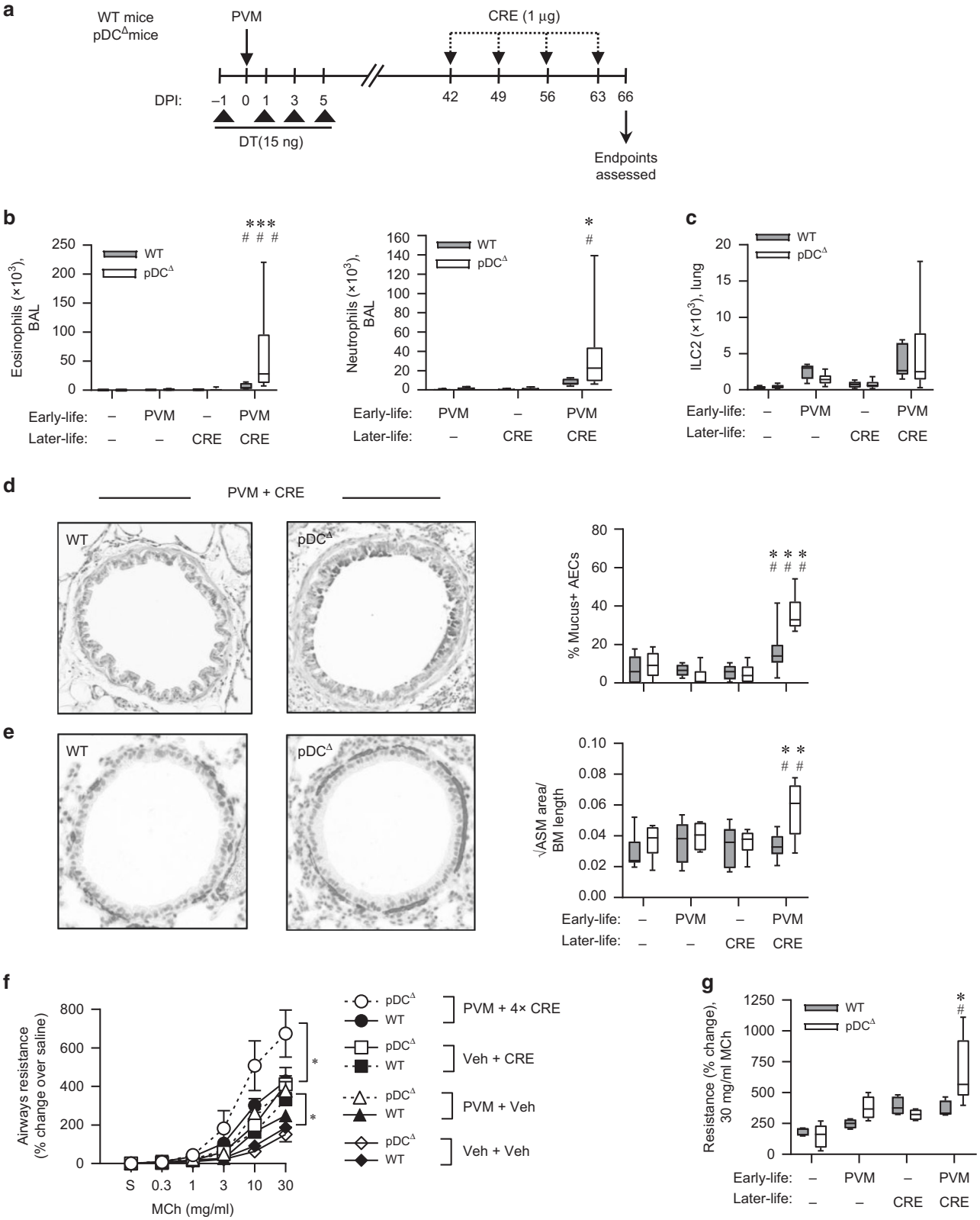

Fig. 1 Severe bronchiolitis in pDC$^{\Delta}$ mice predisposes toward allergen induced asthma. a Study design. **b** Eosinophils and neutrophils in bronchoalveolar lavage (BAL). **c** ILC2s in lung. **d** Mucus producing airway epithelial cells (AECs): representative micrographs (×400 magnification) (left); quantification (right). **e** Airway smooth muscle (ASM) area: representative micrographs (×400 magnification) (left); quantification (right); Airway hyperreactivity (AHR): dose-response to methacholine **f**; resistance at 30 mg/mL methacholine **g**. Data are representative of 6–8 mice per group performed twice and presented as box and whisker plots showing quartiles (boxes) and range (whiskers) (**b**–**e**, **g**) or mean ± SEM (**f**). Asterisk (*) denotes $p < 0.05$, $^{**}p < 0.01$, and $^{***}p < 0.001$ compared to WT mice administered PVM and 4× CRE or as indicated. $^{\#}p < 0.05$, $^{\#\#}p < 0.01$, and $^{\#\#\#}p < 0.001$ compared to pDC$^{\Delta}$ mice administered vehicle diluent.

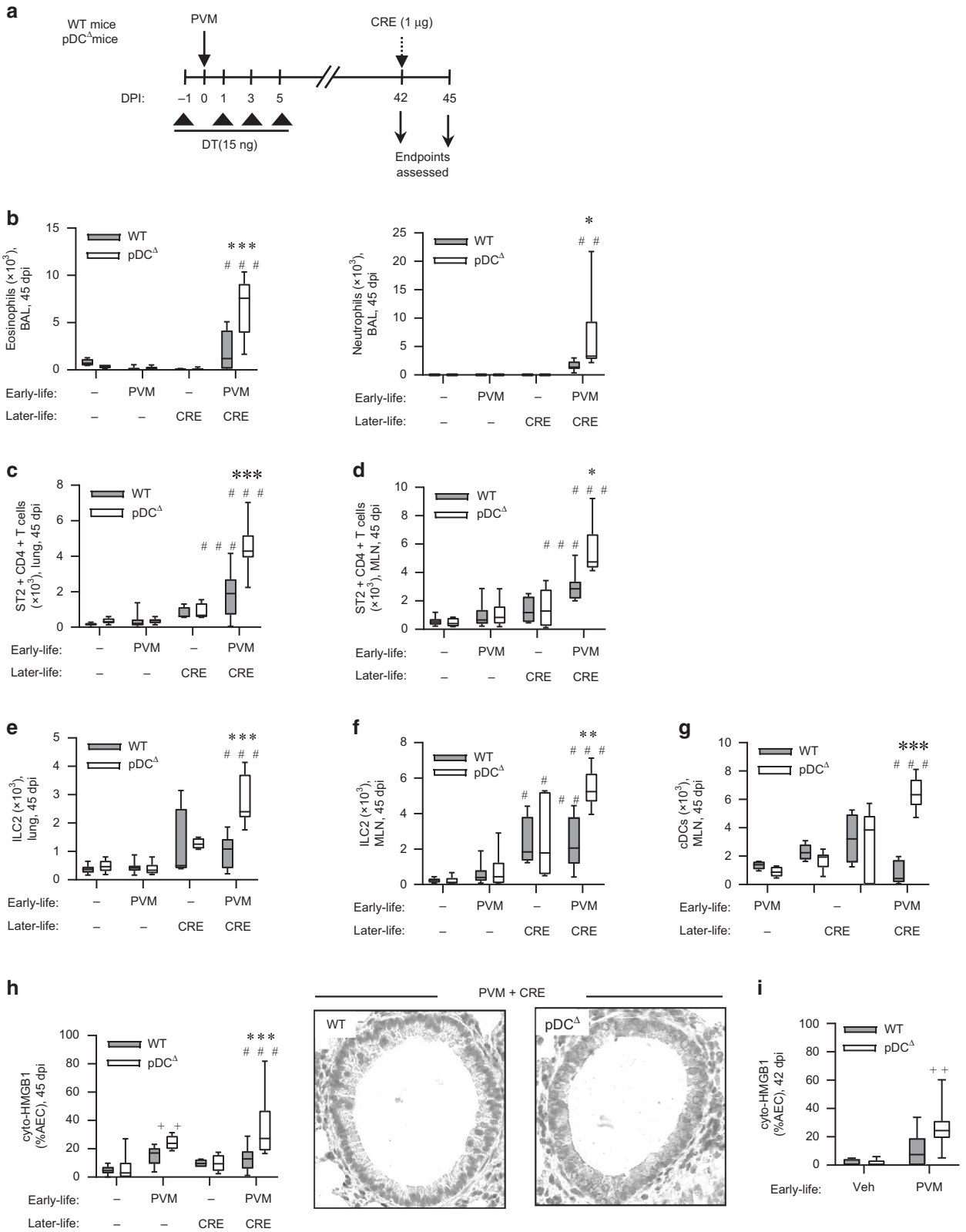

Fig. 2 Severe bronchiolitis in pDC$^{\Delta}$ mice sensitizes to aeroallergen. a Study design. **b** Eosinophils and neutrophils in BAL. ST2^{hi} CD4+ T cells in lung (**c**) and mediastinal lymph node (MLN) (**d**). ILC2s in lung (**e**) and MLN (**f**). Conventional [c]DCs (F4/80−, CD11c+, CD11b+, MHCII+, and CD64−) in MLN (**g**). AEC cytoplasmic HMGB1: **h** quantification at 45 dpi (left panel), representative micrographs (×400 magnification) (right panel); **i** quantification at 42 dpi. Data are representative of six mice per group performed twice and presented as box and whisker plots showing quartiles (boxes) and range (whiskers). *$p < 0.05$, **$p < 0.01$, and ***$p < 0.001$ compared to WT mice administered PVM and 1× CRE. $^{\#}p < 0.05$, $^{\#\#}p < 0.01$, and $^{\#\#\#}p < 0.001$ compared to pDC$^{\Delta}$ mice administered vehicle diluent. $^{+}p < 0.05$, $^{++}p < 0.01$, and $^{+++}p < 0.001$ compared to WT mice administered PVM.

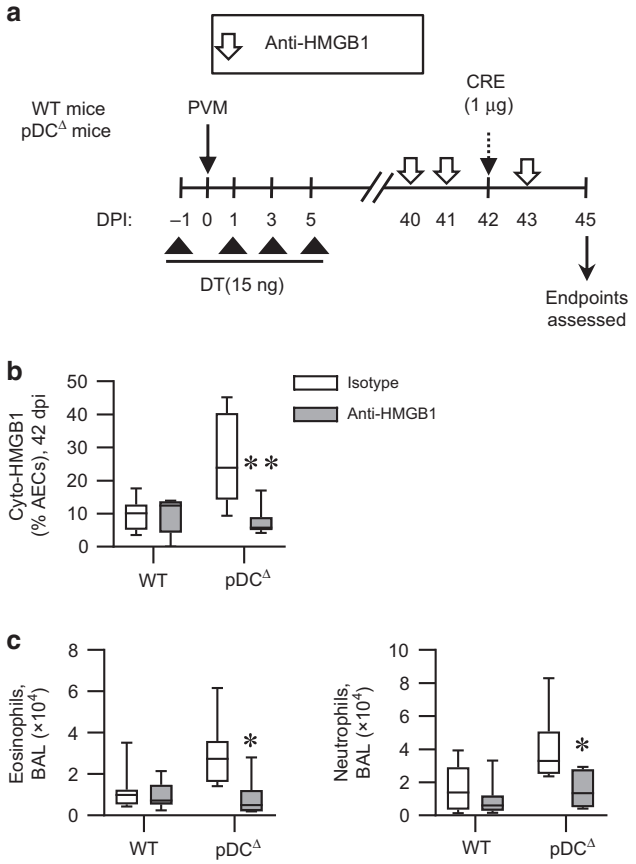

Fig. 3 Severe viral bronchiolitis predisposes to allergic sensitization through HMGB1. a Study design. **b** AEC cytoplasmic HMGB1 quantification at 45 dpi. **c** Cell counts in BAL.

pDC$^{\Delta}$ mice. The same phenotype was observed in the pDC$^{\Delta}$ mice following CRE exposure (Fig. S3a; see study design Fig. 2a). Greater Treg cell numbers in the diseased mice seemed counter-intuitive, however, at 7 days post-secondary viral infection, when asthma-like pathologies develop in this model, the ratio of ST2+ CD4+ T cells to Nrp1+ Treg cells was significantly greater in the pDC$^{\Delta}$ mice (Fig. 5c), suggesting that the Treg cells were not suppressing CD4+ Th2 cell expansion. Indeed, mirroring our findings in the primary infection,[20] ICOS, Lag3, CTLA-4, and TIGIT were not different between the two groups (Fig. 5d) whereas, CD39 expression was significantly lower on Nrp1+ Treg cells in pDC$^{\Delta}$ mice compared to WT mice. Phenotypically, the Nrp1+ Treg cells in the re-infected WT or pDC$^{\Delta}$ mice expressed high (and similar) levels of CD11a and CD44 consistent with a memory/antigen specific response (Fig. S3b).[26] In contrast, these markers were minimally expressed on Treg cells in age-matched adult mice experiencing a primary infection. To confirm that Treg cells generated in the primary infection are long-lived, we FACS-purified Treg cells (CD4^{+}, Nrp1+, FoxP3-RFP^{+}, and >95%) from the MLN of neonatal double transgenic pDC$^{\Delta}$ FoxP3-RFP (red fluorescent protein) mice at 7 dpi, then adoptively transferred (i.p. route) these Treg cells (30×10^3) to recipient pDC$^{\Delta}$ mice at 7 dpi. Upon secondary infection, RFP+ Treg cells were detectable in the MLNs (Fig. S3c, d), indicating that Treg cells from the primary infection persist until the secondary infection.

The absence of pDC in early life leads to long-lived Treg cells that fail to prevent allergen induced asthma

The failure to control ST2+ CD4+ T cell expansion and the lower CD39 expression suggested that the susceptibility of post-bronchiolitic pDC$^{\Delta}$ mice to develop asthma stems from a failure to adequately control airway inflammation upon CRE exposure or secondary viral infection. To test this hypothesis, at 3 days post-secondary infection (45 dpi; Fig. 6a), Treg cells from the MLN of pDC$^{\Delta}$ FoxP3-RFP or WT FoxP3-RFP mice were FACS-purified (Fig. S3d) and adoptively transferred to recipient post-bronchiolitic pDC$^{\Delta}$ mice prior to the induction of CRE-induced or virus-induced experimental asthma. As expected, the transfer of "healthy" Treg cells (i.e., from WT mice) prevented the onset of experimental asthma in susceptible pDC$^{\Delta}$ mice (Fig. 6b–e). In stark contrast, aberrant Nrp1+ Treg cells, sourced from pDC$^{\Delta}$ mice, were incapable of preventing CRE-induced asthma (Fig. 6b–e). Th2 cytokine expression was not assessed as their concentration was below the limit of detection at this time point Fig. 7.

The absence of pDC in early life leads to long-lived Treg cells that fail to prevent allergic sensitization

We hypothesized that the heightened susceptibility to allergen-induced asthma in pDC$^{\Delta}$ mice is underpinned by the failure of aberrant Treg cells to prevent sensitization. Consistent with this theory, at three days post CRE (Fig. 7a), the transfer of "healthy" Treg cells (from WT mice) diminished granulocytic inflammation (Fig. 7b) and lowered ST2+ CD4+ T cells and ILC2 numbers in the lungs and MLNs (Fig. 7c–f). In contrast, "diseased" Treg cells (from pDC$^{\Delta}$ mice) were incapable of preventing CRE-induced airway inflammation (Fig. 7b–f). In keeping with the attenuated T cell response, adoptive transfer of healthy but not diseased Treg cells decreased cDC numbers in the MLNs (Fig. 7g). Interestingly, the ability of Nrp1+ Treg cells isolated from WT mice, but not pDC$^{\Delta}$ mice, to suppress airway inflammation was associated with a significant reduction in cytoplasmic HMGB1 expression in AECs (Fig. 7h).

Long-lived aberrant Treg cells fail to prevent asthma progression to viral re-challenge

To address whether the generation of defective Treg cells in early-life increases susceptibility to later virus-associated asthma, we repeated the adoptive Treg cell transfer model, and challenged the pDC$^{\Delta}$ recipients with PVM (Fig. 8a). Again, "healthy" Nrp1+ Treg cells (from WT mice) were effective in suppressing virus-induced experimental asthma in pDC$^{\Delta}$ mice (Fig. 8b–e) at 49 dpi. In contrast, "diseased" Treg cells (from pDC$^{\Delta}$ mice) were unable to prevent asthma development. As with CRE exposure, re-infection induced an increase in the fraction of cytoplasmic HMGB1 expressing AECs, a response that was significantly greater in the post-bronchiolitic pDC$^{\Delta}$ mice (Fig. 8f). Strikingly, this hyper-active epithelial response was attenuated following the adoptive transfer of healthy but not diseased Nrp1+ Treg cells (Fig. 8g).

Dysfunctional Treg cells fail to suppress allergen-induced HMGB1 translocation in AECs

Treg cells can suppress T cell activation either directly or indirectly, for example via the induction of tolerogenic DCs. In light of the suppressive effects of Treg cells on allergen-induced and virus-induced HMGB1translocation in AECs, and our previous work identifying an important role for epithelial HMGB1 in the induction of type-2 airway inflammation,[4] we postulated that the Treg cells prevent airway eosinophilia and airway remodeling by acting directly on the airway epithelium. To explore this possibility, we first isolated mouse AECs from naïve WT mice, cultured the undifferentiated cells until confluent, and confirmed that CRE (1 µg) exposure induces a time-dependent nuclear-to-cytoplasmic translocation of HMGB1 (Fig. 9a). We next isolated Nrp1+ Treg cells from WT or pDC$^{\Delta}$ mice at 45 dpi (as per the in vivo transfer model) and co-cultured these Treg cells at various ratios with the mouse AECs. Whereas "healthy" Treg cells suppressed CRE-induced HMGB1 translocation, "diseased" Treg cells were significantly less effective at dampening this response (Fig. 9b). These data suggest that the generation of impaired Treg cells in early-life

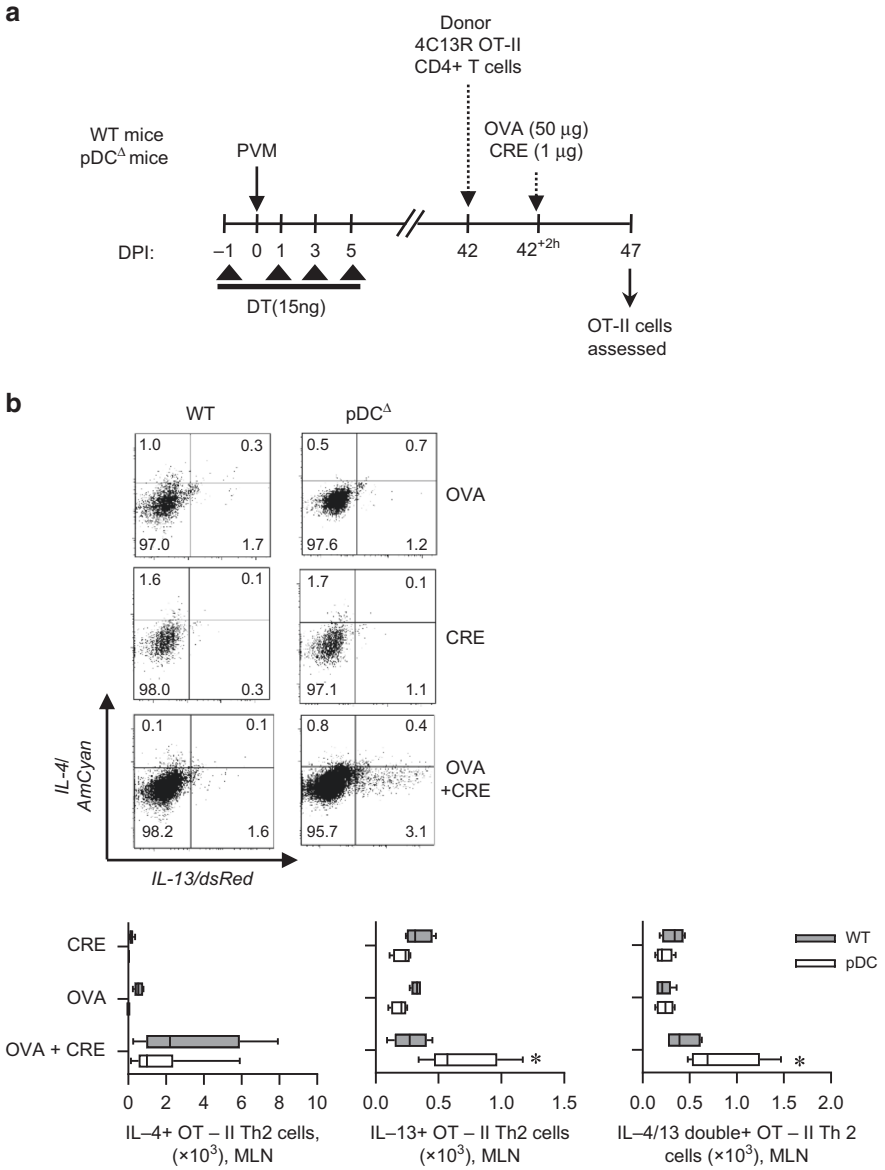

Fig. 4 Severe viral bronchiolitis predisposes to allergic sensitization through bystander CD4+ Th2 cell activation. a Study design. **b** Representative FACS plots (top). Numbers of OT-II T cells expressing IL-4/AmCyan (bottom left), IL-13/dsred (bottom middle) and both IL-4/13 (bottom right). Data are representative of five mice per group performed twice and presented as box and whisker plots show quartiles (boxes) and range (whiskers). *$p < 0.05$, **$p < 0.01$, and ***$p < 0.001$ compared to WT mice administered OVA and CRE.

contributes to asthma progression by failing to limit epithelial cell-mediated inflammation.

DISCUSSION

The persistent and aberrant inflammatory response that promotes the pathophysiology of asthma occurs as a consequence of insufficient immunoregulation. Fundamental to balancing the magnitude and duration of inflammatory responses, Treg cells have been shown to be defective in asthma patients of all age groups, all subtypes, and during acute exacerbations.[1] However, the underlying causes and events that give rise to this state of Treg cell hypo-responsiveness remain elusive. Here, we reveal that Treg cells generated in early life are long-lived, and that their programming as competent or incompetent suppressor cells heavily influences host sensitization and experimental asthma upon later exposure to allergen or respiratory virus. Furthermore, we identify that the post-bronchiolitic airway epithelium is functionally altered, leading to a heightened innate response that facilitates Th2 cell priming, and that healthy Treg cells can directly suppress this aberrant epithelial response. Altogether, our findings show that consequent to a defect in the pDC compartment in infancy, a respiratory virus infection leads to the generation of functionally impaired, long-lived Treg cells and a hypersensitive airway epithelium, that together, predispose to the development of later asthma. Thus we provide a cellular and molecular explanation for the association between severe viral bronchiolitis in infancy and the subsequent development of asthma.[13,14]

In patients with established asthma, the airway epithelium is structurally and functionally abnormal, potentially as a consequence of excessive tissue damage and repeated repair processes.[27] More recently, the epithelium has been implicated as an orchestrator of Th2 immunity via DC recruitment and activation, and an ability to produce Th2 "instructive" cytokines, such as IL-33 and HMGB1.[3–5] Herein we identify that the severity of bronchiolitis in infancy markedly affects the mucosal immune

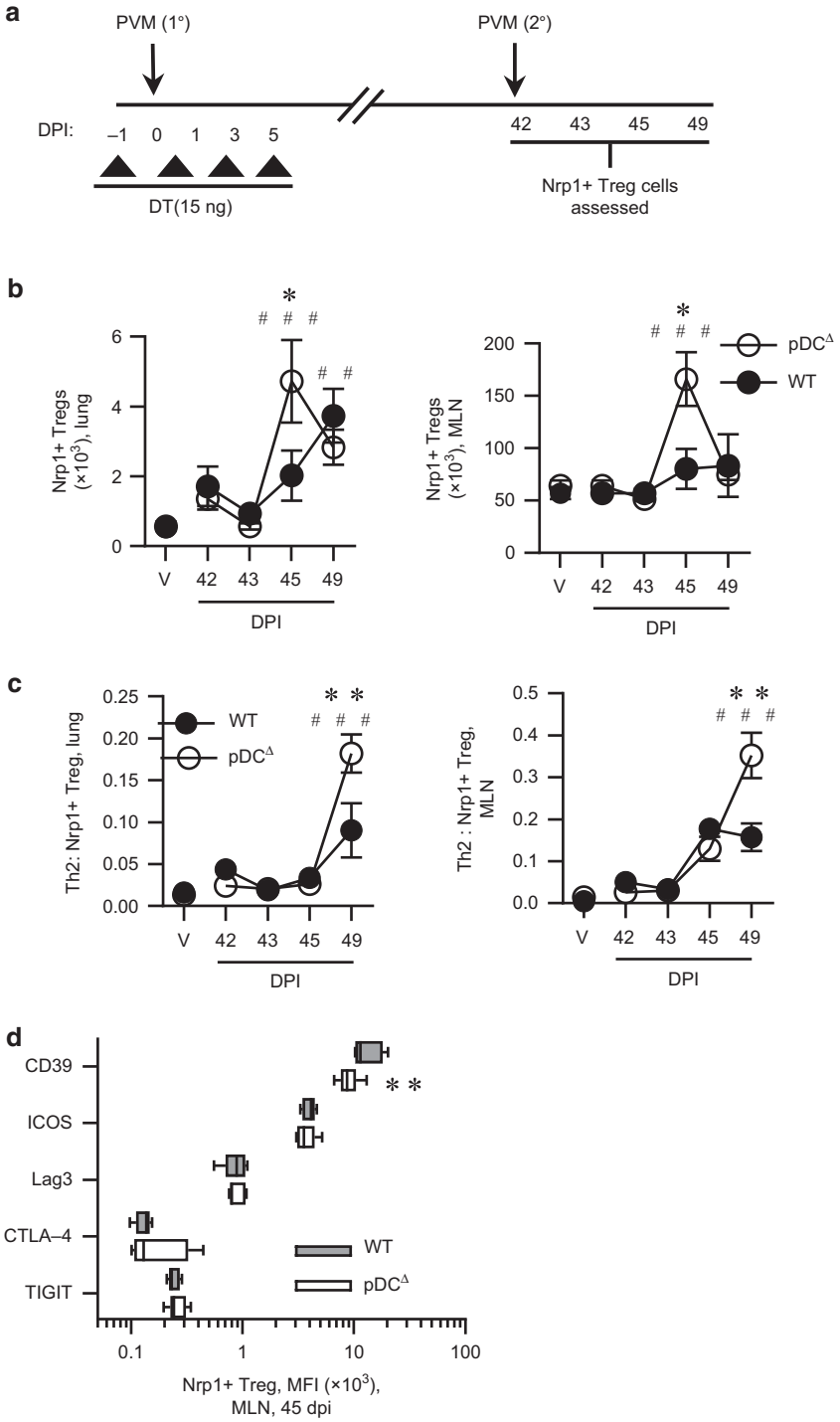

Fig. 5 Defective Treg cells generated in early-life persist and remain impaired in later-life. a Study design. **b** Nrp1+ Treg cell number in lung (left) and MLN (right). **c** Ratio of Th2 ($ST2^{hi}$ CD4+ T cells) to Nrp1+ Treg cells in lung (left) and MLN (right). **d** Expression of suppressive markers on Nrp1+ Treg cells in MLN. Data are representative of 6–8 mice per group performed twice and presented or mean ± SEM (**b**, **c**) or as box and whisker plots showing quartiles (boxes) and range (whiskers) (**d**). $^{*}p < 0.05$, $^{**}p < 0.01$, and $^{***}p < 0.001$ compared to WT mice administered PVM 2×. $^{\#}p < 0.05$, $^{\#\#}p < 0.01$, and $^{\#\#\#}p < 0.001$ compared to pDC^{Δ} mice administered vehicle diluent.

response to CRE allergen in later-life. Thus, mice that had experienced severe bronchiolitis present with significantly greater numbers of eosinophils, ST2+ CD4+ T cells, ILC2s and cDCs in the airway mucosa or MLNs, and more readily promoted the differentiation of antigen-activated naïve CD4 T cells towards CD4+ Th2 cells. Strikingly, this enhanced susceptibility to initiate type-2 inflammation was associated with an elevated number of activated AECs, as assessed by cytoplasmic HMGB1 expression. Indeed, this phenotype was evident even in the absence of CRE exposure, indicating that severe viral infection in early life induces long-lived changes in the airway mucosa. Whether these changes are intrinsic to the airway epithelium, as has been reported in the context of IL-33 expression following Sendai virus infection,[28] or occur secondarily to the actions of a tissue resident immune cell

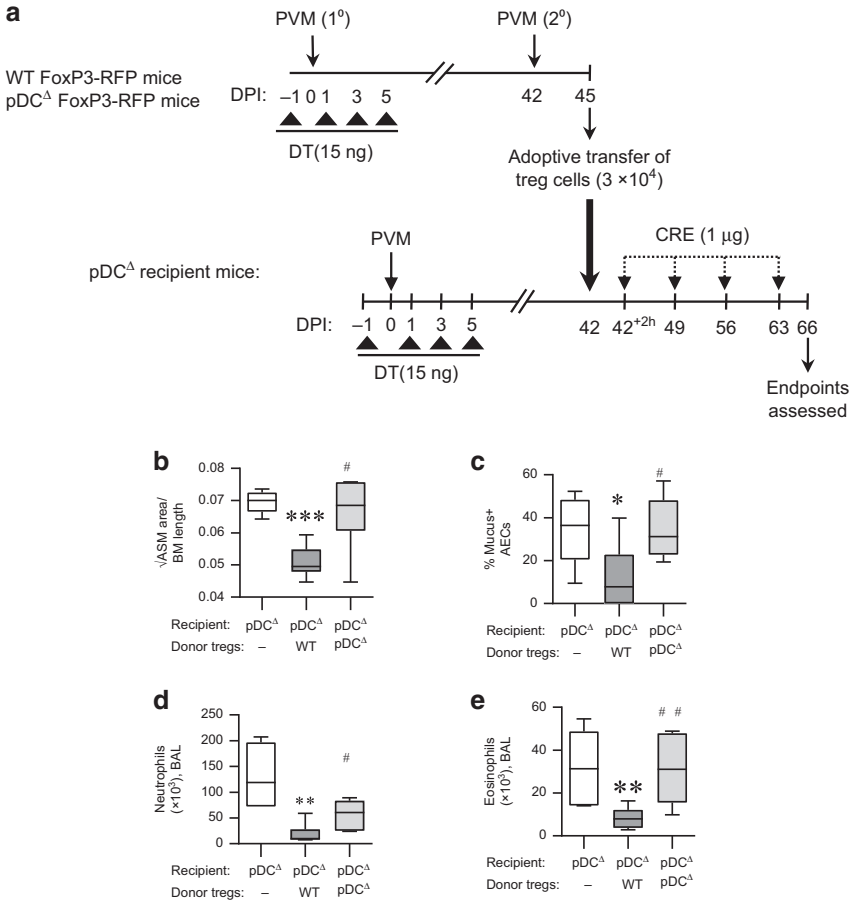

Fig. 6 The absence of pDC in early life leads to long-lived Treg cells that fail to prevent allergen induced asthma. a Study design. **b** ASM area. **c** Mucus producing AECs. Neutrophils (**d**) and eosinophils (**e**) in BAL. $^{*}p < 0.05$, $^{**}p < 0.01$, $^{***}p < 0.001$ compared to WT re-infected mice or as indicated. $^{\#}p < 0.05$, $^{\#\#}p < 0.01$, $^{\#\#\#}p < 0.001$ compared to pDC$^{\Delta}$ re-infected mice.

remains to be determined. However, there is an emerging appreciation that respiratory and skin epithelial progenitor cells can acquire "memory" in response to IL-4/IL-13 or IL-1 signaling,[29,30] pathways that are elevated in severe bronchiolitis,[5,31–33] and which may, therefore, contribute to the phenotype observed in our model.

Treg cells are fundamental to the induction of tolerance to inhaled allergens,[34,35] and are critical for the regulation of innate and adaptive responses to secondary insults.[36,37] We previously demonstrated that pDCs are critical for the expansion of functional Tregs during neonatal PVM infection.[20] Notably, pDCs supported Treg cells through the provision of Sema4a and not the production of type I IFNs. In the present study, we show that mice that experienced mild, but not severe, bronchiolitis were resistant to later allergen-induced asthma. This raised the possibility that protection against allergic sensitization and asthma development was conferred by long-lived Treg cells generated in infancy. Consistent with this, the Treg cells that expanded upon secondary infection expressed low levels of CD39, mirroring our previous findings in the primary infection.[20] Also, the magnitude of Treg cell expansion was increased in the pDC$^{\Delta}$ mice, similar to that shown by CTLA4-deficient Treg cells, which are also functionally impaired. In healthy WT mice, Treg cell expansion was far smaller, possibly due to the milder inflammatory response in the airways, a notion that is supported by the lower Th2/Treg ratio. We confirmed that Treg cells generated during the primary infection can persist until the reinfection by transplanting FoxP3-RFP Treg cells in early-life. Although the numbers of Treg cells in the lymph node after reinfection was small, it must be appreciated that the majority of donor cells are known to die following transplant, and of those that survive, the majority would contract further upon transition to memory Treg cells.[38]

Several investigators have shown that the adoptive transfer of healthy Treg cells or their boosting by immunomodulatory products is sufficient to ameliorate experimental asthma.[39] We found that the transfer of healthy Treg cells to "at risk" post-bronchiolitic pDC$^{\Delta}$ recipients prevented the development of CRE-induced or virus-induced asthma, even though the Treg cells were expanded in response to secondary PVM infection. This non-antigen specific suppression may partly explain the human epidemiology linking severe viral bronchiolitis with later allergic sensitization and asthma. In other words, the programming of functional Treg cells during RSV infection in infancy protects the host from generating inappropriate T cell response to other airway exposures in later-life. In direct support of this, we show that long-lived Treg cells generated in the absence of pDCs during a respiratory viral infection in early life are incapable of preventing allergic sensitization or viral-induced asthma in a susceptible host in later life.

HMGB1 has been shown to be a key upstream regulator of neutrophils, ILC2, and DCs, which work collaboratively to prime naive T cells and potentiate memory Th2 responses.[4,40,41] However, of these cell types, anti-HMGB1 only affected neutrophil numbers during the "sensitization phase". A limitation of our study is that we did not address whether HMGB1 blockade was sufficient to prevent the development of asthma. Notably, the adoptive transfer of healthy but not aberrant Treg cells significantly lowered the fraction of cytoplasmic HMGB1 positive

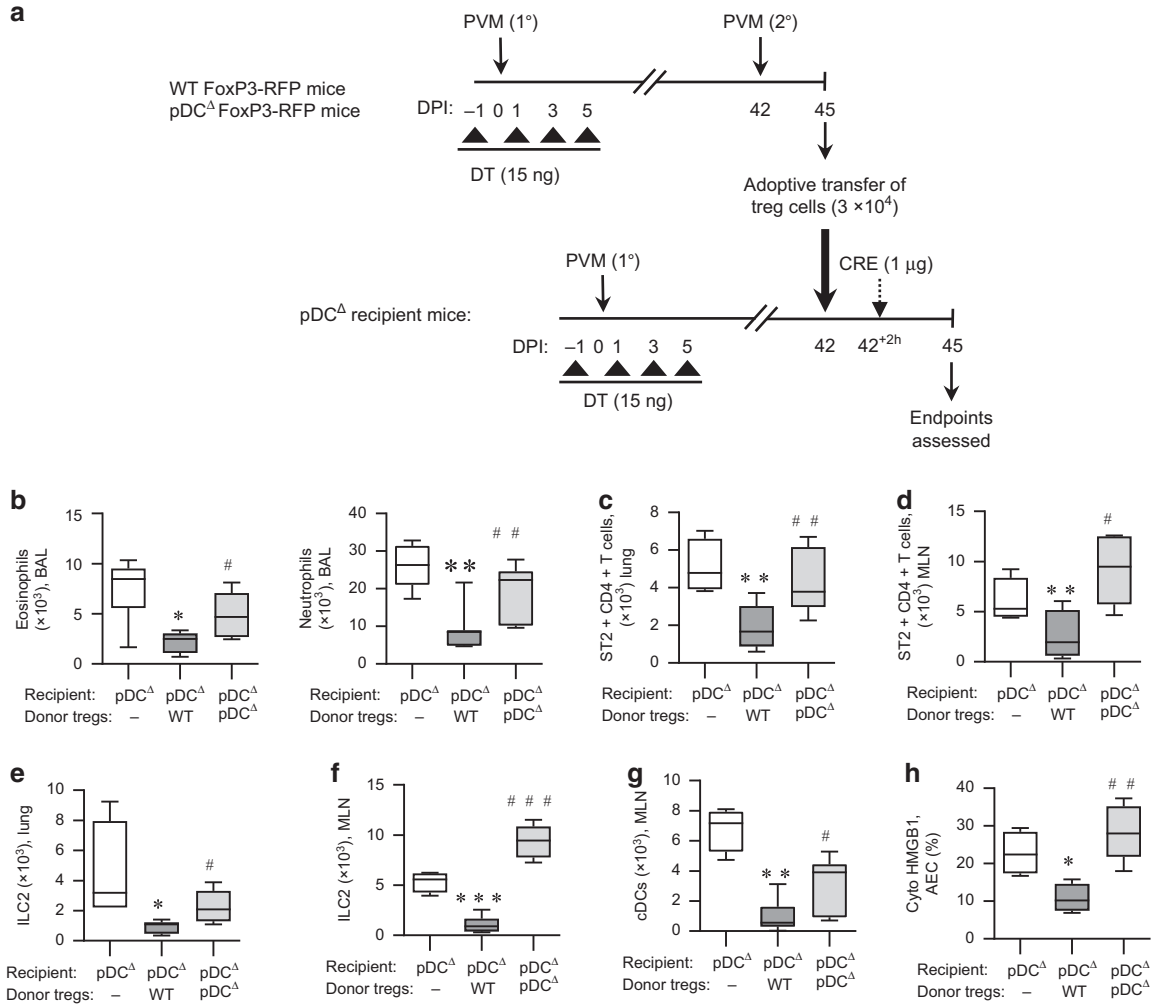

Fig. 7 The absence of pDC in early life leads to long-lived Treg cells that fail to prevent allergic sensitization. a Study design. **b** Eosinophils and neutrophils in BAL. ST2^{hi} CD4+ T cells in lung (**c**) and MLN (**d**). ILC2s in lung (**e**) and MLN (**f**). **g** cDCs in MLN. **h** Cytoplasmic HMGB1 quantification. Data are representative of five mice per group performed twice and presented as box and whisker plots show quartiles (boxes) and range (whiskers). *$p < 0.05$, **$p < 0.01$, and ***$p < 0.001$ compared to WT mice administered PVM and 1× CRE. $^{\#}p < 0.05$, $^{\#\#}p < 0.01$, and $^{\#\#\#}p < 0.001$ compared to pDC$^{\Delta}$ mice that received WT Nrp1+ Treg cells.

airway epithelial cells in vivo, and attenuated neutrophilic inflammation following CRE exposure. Thus, we speculate that healthy Treg cells confer protection against allergic sensitization by suppressing HMGB1-induced neutrophilia. In support of this concept, we demonstrated in an in vitro co-culture model that healthy but not aberrant Treg cells suppress CRE-induced HMGB1 translocation in mouse AECs. Nrp-1+ Treg cells primarily suppress inflammatory responses via the production of soluble factors, and although we did not detect differences in IL-10 or amphiregulin levels in the co-culture model (data not shown), a non-contact dependent mechanism of suppression is most likely active given the vast numbers of epithelial cells lining the airways. Altogether, our findings suggest that the generation of functionally impaired Treg cells in early life affects epithelial responsiveness to an unrelated allergen in later-life, and that this affects a critical threshold that tips the balance between tolerance and the development of allergic sensitization.

A limitation of our study is that we did not identify the mechanism by which Treg cells attenuate alarmin release, although we speculate that CD39 contributes by hydrolyzing ATP to adenosine. Additionally, we were unable to detect Th2 cytokines (e.g., IL-5) in the BALF as we sampled 72 h after the final CRE challenge, and our preference is to use a clinically relevant allergen at low dose rather than a supramaximal dose, which can generate artefacts. We and others have shown that IL-33 is an important mediator of type 2 inflammation,[4,5,42,43] and although we did not detect elevated IL-33 in this model, it may play an active role in driving the type 2 inflammatory response observed. Importantly, however, our model of experimental asthma induced the hallmark features of asthma, including ASM remodeling. Collectively, our findings provide a unifying hypothesis to explain the association between severe viral infection in early-life and the subsequent development of allergic sensitization and asthma, low circulating pDC numbers in infancy, and impaired Treg cell function in asthma.[44] Our data further implicate a causal relationship between severe bronchiolitis and later asthma and highlight a novel developmental origin of asthma that stems from a dysregulated pDC-Treg cell axis in infancy.

METHODS

Mouse strains and treatments

BDCA-2-DTR,[45] OT-II 4C13R, C57BL/6, and FoxP3-RFP[46] mice were maintained under specific pathogen free conditions at the Australian Institute of Biotechnology and Nanotechnology Animal Facility (The University of Queensland) and the QIMR Berghofer

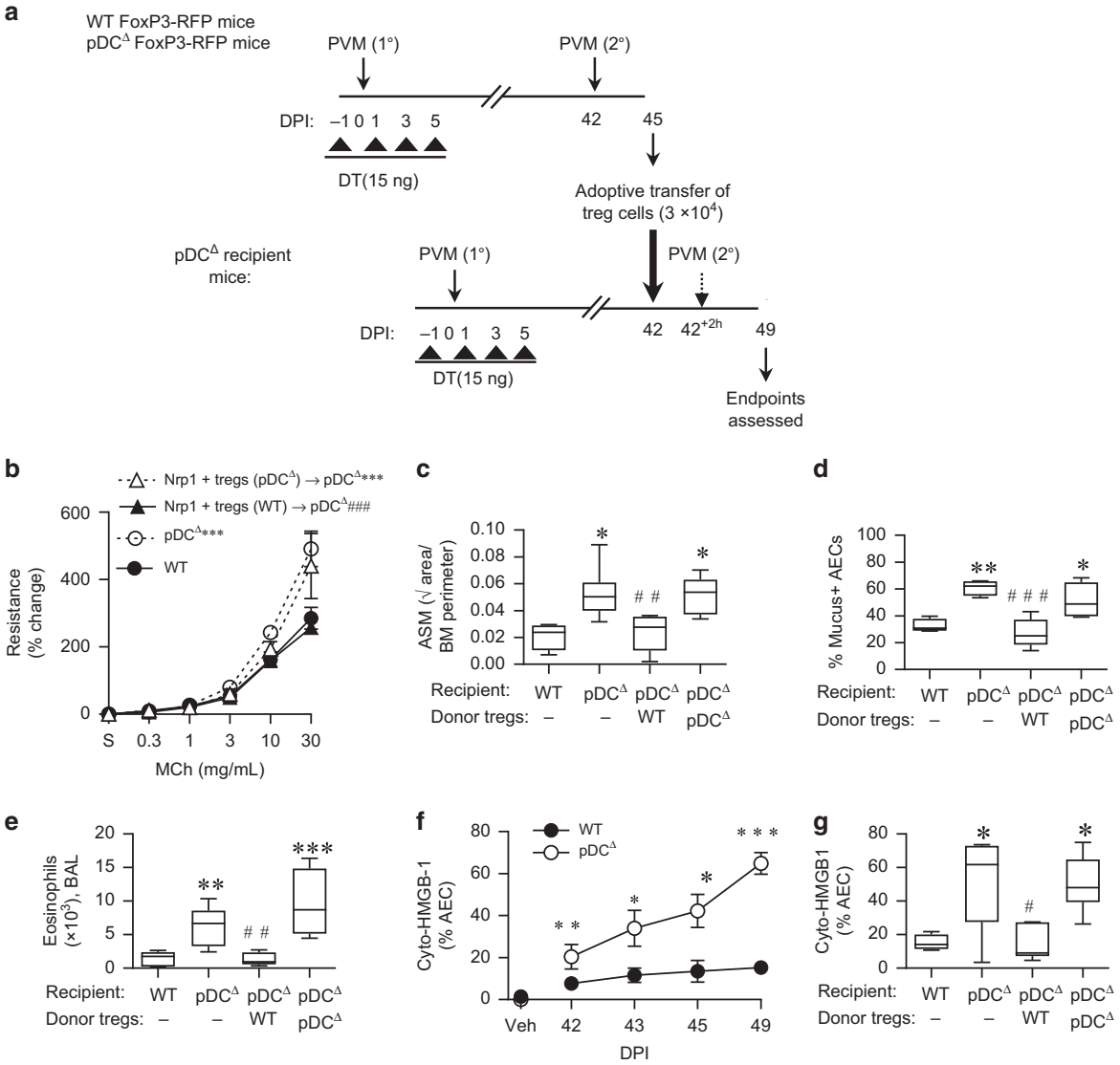

Fig. 8 Long-lived aberrant Treg cells fail to prevent asthma progression to viral re-challenge. a Study design. **b** AHR. **c** ASM area. **d** Mucus producing AECs. **e** Eosinophils in BAL. AEC cytoplasmic HMGB1 (**f**, **g**). $^{*}p < 0.05$, $^{**}p < 0.01$, and $^{***}p < 0.001$ compared to WT re-infected mice or as indicated. $^{\#}p < 0.05$, $^{\#\#}p < 0.01$, and $^{\#\#\#}p < 0.001$ compared to pDC$^{\Delta}$ re-infected mice.

Medical Research Institute Animal Facility. Neonatal mice generated from time mating of BDCA2-DTR with C57BL/6 mice or FoxP3-RFP mice were genotyped by standard PCR using primers against *hGH* (BDAC-2-DTR mice) forward, 5′-GCCCCCGGGCAGC ACAGCCACTGCCGGTCC-3′ and reverse, 5′-GGCCAAGCGCTTGGG CACTGTTCCCTCCCT-3′; *Dsred* (4C13R mice), forward, 5′-GCTC CAAGGTGTACGTGAAG-3′ and reverse, 5′-GCTTGGAGTCCACGTAG TAG-3′; FoxP3-RFP mice mutant, 5′-GGAATGCTCGTCAAGAAGA CAGG-3′ and common, 5′-CAA AAC CAA GAA AAG GTG GGC-3′ and wild type, 5′-CAG TGC TGT TGC TGT GTA AGG GTC-3.′ OT-II mice carrying a transgenic T cell receptor specific for I-A^{b}/ OVA$_{323-339}$ mice were genotyped based on expression of MR9-4 and BD20.1 by FACS analysis. Neonatal BDCA2-DTR transgene positive (denoted pDC$^{\Delta}$) and negative (denoted WT) littermate controls received a low dose (15 ng) of diphtheria toxin (DT; Calbiochem, San Diego CA) by intraperitoneal (i.p.) injection at −1, 1, 3, and 5 days post infection (dpi).[20] DT administration with these protocols was routinely confirmed to induce >90% depletion of pDCs until 7 dpi. DT did not induce any adverse effects, or induce an immune response in the absence of infection.[20] In some studies, mouse anti-HMGB1 (R&D Systems, AF1690) or isotype control (3 µg in 50 µL PBS, R&D Systems) was administered at the time points stated. All experiments were approved by The University of Queensland Animal Ethics Committee and the QIMR Berghofer Animal Ethics Committee.

PVM inoculation and allergen administration

Pneumonia virus of mouse stock J3666 was prepared as previously described.[33] PVM or vehicle diluent (Dulbecco's Modified Eagle Medium, DMEM/ fetal bovine serum, FBS, 10% v/v, Gibco, Gaithersburg, MD) was administered intranasally (i.n.) in 10 µL on day 7 of life (10 plaque forming units, PFU) under light isoflurane-induced anesthesia as previously described.[47] At 42 dpi, 100 PFU of PVM, cockroach extract (Greer; CRE; 1 µg in PBS) or LPS-free OVA (50 µg in PBS) was administered i.n. in 50 µL. In some experiments, 1 µg of CRE was administered a total of four times at 42, 49, 56, 63 dpi.

Flow cytometry

The left lung lobe and the smallest postcaval lobe or the MLN were washed in PBS/2% FCS before mechanical dissociation using a pestle and a 70 µm cell strainer (BD Biosciences, San Jose, CA).

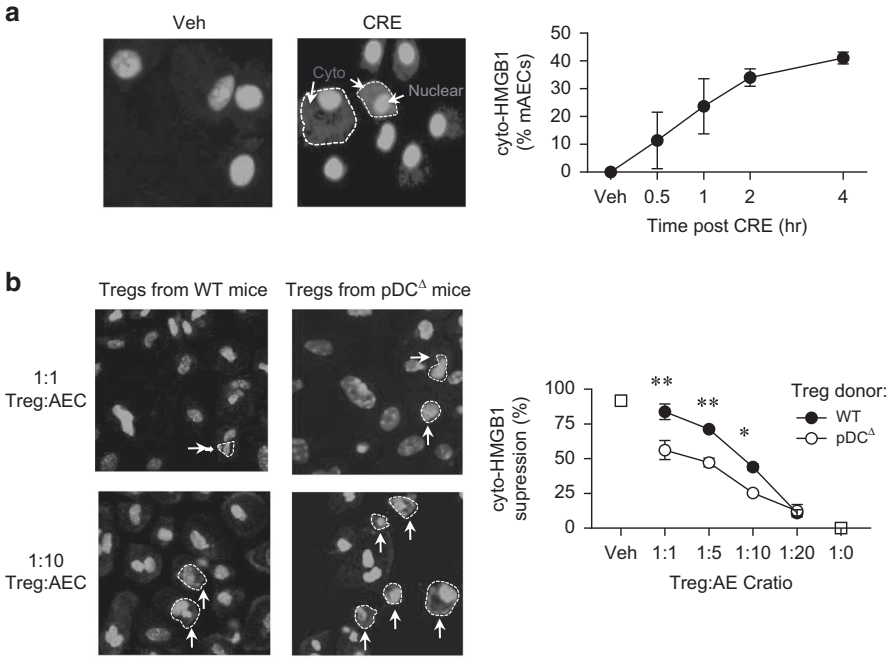

Fig. 9 Dysfunctional Treg cells fail to suppress allergen-induced HMGB1 translocation in AECs. a HMGB1 immunostaining (left). mAECs (%) expressing cytoplasmic HMGB1 (right). **b** HMGB1 immunostaining (left). Suppression of AEC cytoplasmic HMGB1 by Nrp1+ Treg cells at 4 h post CRE, expressed as % suppression relative to CRE-treated AECs alone (right). Data are representative of 6–8 mice per group performed twice and presented as mean ± SEM. *$p < 0.05$, **$p < 0.01$, and ***$p < 0.001$ compared to pDC$^{\Delta}$ Nrp1+ Treg cells (**a**) or CRE treated mAECs (**b**).

Isolated single cell suspensions were washed with PBS/2% FCS and red blood cells lysed using Gey's buffer. Cells were washed again followed by incubation with anti-FcγRIII/II (Fc block) for 15 min at 4 °C. Cells were stained using fluorescently labeled antibodies directed against CD4-APCCy7, CD4-AF488 or CD4-V500 (RM4-5), Ly6G-FITC (1A8), CD8α-PerCP-Cy5.5 (53-6.7), Gr-1–AF488 (RB6-8C5), CD11b–AF488 (M1/70), B220-AF488 (RA36B2), (all BD Bioscience, San Jose, CA), CD25-BV605 (PC61), CD3ε-AF488 (145.2CII), CD19-AF488 (6D5), CD45-BV421 (30-F11), CD11b-BV421 (M1/70), ST-2-APC (DIH9), MR9-4 (TCR V beta 5, AlexaFluor647) and BD20.1 (TCR V alpha 2, PerCP-Cy5.5) (all Biolegend, San Diego, CA), neurophilin-1-AF488 (761705; R&D Systems, Minneapolis, MN), CTLA-4-PE (UC10-4B9), CD39-PerCP-efluor710 (24DMS1), ICOS-PE (C398.4A), Lag3-PerCP-efluor710 (C9B7W), TIGIT-PE (GIGD7), PD-1-APC-780 (J43). 7-AAD (eBioscience, San Diego, CA), Zombie Aqua or Zombie NIR (Biolegend, San Diego, CA) were used to exclude dead cells. For intracellular staining, cells were fixed and permeabilized using the BD Cytofix/Cytoperm™ Kit as per the manufacturer's instructions (BD Biosciences, San Jose, CA) and stained with FoxP3-AlexaFluor 647 or PE, (MF23; BD Biosciences, San Jose, CA). Stained cells were washed and acquired on a BD LSRFortessa X-20 (BD Biosciences, San Jose, CA) and analyzed using FACS Diva Software v8 (BD Biosciences, San Jose, CA) and FlowJo v8.8 (Tree Star Inc., Ashland, OR).

Cell sorting

For adoptive transfer experiments Nrp1+ Treg cells (Nrp-1^{+}, CD4^{+}, FoxP3-RFP^{+}) were isolated from the MLN of PVM-infected FoxP3-RFP mice or FoxP3-RFP pDC$^{\Delta}$ mice at the time points indicated (see Study designs). Single cell suspensions were generated by digestion of lung tissue using a gentleMACS (Miltenyi Biotec) as per the manufacturer's instructions and the RBCs were lysed with Gey's buffer. Cells were then washed, blocked with Fc Block and fluorochrome-labeled antibodies as described before enrichment using the EasySep™ Mouse CD4+ T Cell Isolation Kit (StemCell). Zombie-NIR^{-}, Nrp-1^{+}, CD4^{+}, FoxP3-RFP^{+} Treg cells were sorted on a BD FACSAria Fusion. The purity of FACS sorted cells was >95% of the parent population in all cases. Treg cells (3×10^4) or vehicle diluent (10% FCS/DMEM) were adoptively transferred to individual pDC$^{\Delta}$ or WT mice the same day.

Cell culture

WT mouse tracheal epithelial cells were dissociated using dispase (BD Biosciences) and peeled off using forceps, before culturing in MTEC/Plus on collagen-coated plates, as previously described.[48] Cells were seeded into chamber slides and grown to 80% confluence (approximately 5×10^4 cells/well). Nrp1+ Treg cells from WT or pDC$^{\Delta}$ (isolated at 45 dpi as described above). For Nrp1+ Treg and mAEC co-culture experiments, soluble anti-CD3 (1 µg; Biolegend) and rmIL-2 (100 U/mL; Ebioscience) were added to all wells. Media was collected at indicated times and cells were fixed in 10% formalin for 15 min prior to staining.

Immunohistochemistry and histology

For inflammatory cell counts, BAL was performed as previously described.[20] Briefly, 600 µL of PBS was washed through the lungs using the tubing and adapter from a 20 G catheter (BD) inserted into the trachea. The resultant cell suspension was spun down, and a total cell viability count performed. Cytospins were prepared using a StatSpin Cytofuge, fixed in methanol, stained (May-Grunwald Giemsa) and mounted using DEPEX. A differential cell count was obtained from 300 cells. Paraffin-embedded lung sections were prepared as previously described.[33] For immunostaining, blocking was performed with 10% normal goat serum, 10% rabbit serum or 10% donkey serum in PBS for 30 min. Sections or cells were probed with anti-HMGB1 (Ab 18256, Abcam), anti-α-SM actin (Sigma-Aldrich Primary was incubated overnight at 4 °C. Following incubation with appropriate secondary antibodies, immunoreactivity was developed with Fast Red (Sigma-Aldrich) and counterstained with Mayer's hematoxylin (bright field) or with 4′,6-diamidino-2-phenylindole (DAPI, Sigma-Aldrich) (fluorescence). For bright field, digitally scanned sections were by analyzed using Aperio Image Scope Software (Scanscope XT; Aperio, Vista, CA). Mucus was identified by Periodic acid-Schiff

staining and quantified as PAS + AECs a percentage of the total AECs in airway and expressed as an average of >5 airways. HMGB1 translocation from the nucleus to cytoplasm was quantified as a percentage of all AECs in the airway and expressed as an average of >5 airways or for cultured AECs 300 randomly selected cells. Airway smooth muscle mass around the small airways (defined as a circumference <800 µm) was measured using Scanscope XT software and expressed as area per µm of basement membrane. Images were captured at X40 or X100 magnification with an Olympus microscope (model BX51), a digital camera (Olympus DP70), and DP software (Olympus, Center Valley, PA).

Cytokine analysis

The concentration of mouse IL-5, IL-13, IL-33, and amphiregulin (all R&D Systems), HMGB1 (Chondrex), IL-10, IL-25, TSLP (all Biolegend) was quantified by ELISA.

Measurement of airway hyperreactivity

Mice were mechanically ventilated and airway hyperreactivity to inhaled β-methacholine was determined by alterations in resistance by forced oscillation technique as described previously.[49] Briefly, anesthetized animals were tracheotomized and applied to the Flexivent (SCIREQ). Dose-responses to nebulized methacholine (0.3–10 mg/mL; Sigma-Aldrich) were expressed as the percentage change over saline control (baseline).

Statistical analyses

GraphPad Prism 7.0 software (La Jolla, California) was used for statistical analyses. A Student's *t*-test, one-way ANOVA with a Tukey post-hoc test or two-way ANOVA with Sidak post-hoc test was applied as appropriate. $p < 0.05$ was considered statistically significant. Additional methods and all other chemicals are listed in the Methods section in the Supplementary Information.

ACKNOWLEDGEMENTS

This work was supported by an Australian Infectious Disease Research Excellence Award to S.P., J.P.L., and J.W.U., a Rebecca L. Cooper Medical Research Foundation equipment grant awarded to S.P., an NHMRC grant awarded to S.P. and J.W.U., and an Australian Research Council Future Fellowship to S.P. The authors wish to thank Dr. Marco Colonna, Washington University, for providing BDCA2-DTR mice and Dr. Christian Engwerda, QIMR Berghofer MRI, for providing FoxP3-RFP mice, and staff at the Flow Cytometry Facility, Translational Research Institute, for their assistance with cell sorting.

AUTHOR CONTRIBUTIONS

J.P.L. and S.P. conceived the project. J.W.U., G.R.H., and R.J.S. provided intellectual input and reagents. S.P. and J.P.L. designed the experiments, analyzed and interpreted the data, and prepared the manuscript. J.P.L, R.B.W., B.F.C., I.S., A.A., A.S., and V.Z. performed the experiments.

ADDITIONAL INFORMATION

The online version of this article (https://doi.org/10.1038/s41385-020-0268-8) contains supplementary material, which is available to authorized users.

Competing interests: The authors declare no competing interests.

Publisher's note Springer Nature remains neutral with regard to jurisdictional claims in published maps and institutional affiliations.

REFERENCES

1. Kinoshita, T. et al. Natural regulatory T cells in isolated early responders compared with dual responders with allergic asthma. *J. Allergy Clin. Immunol.* **133**, 696–703 (2014).
2. Ling, E. M. et al. Relation of CD4+CD25+ regulatory T-cell suppression of allergen-driven T-cell activation to atopic status and expression of allergic disease. *Lancet* **363**, 608–615 (2004).
3. Oczypok, E. A. et al. Pulmonary receptor for advanced glycation end-products promotes asthma pathogenesis through IL-33 and accumulation of group 2 innate lymphoid cells. *J. Allergy Clin. Immunol.* **136**, 747–756 (2015).
4. Ullah, M. A. et al. Receptor for advanced glycation end products and its ligand high-mobility group box-1 mediate allergic airway sensitization and airway inflammation. *J. Allergy Clin. Immunol.* **134**, 440–450 (2014).
5. Lynch, J. P. et al. Aeroallergen-induced IL-33 predisposes to respiratory virus-induced asthma by dampening antiviral immunity. *J. Allergy Clin. Immunol.* **138**, 1326–1337 (2016).
6. Hinks, T. S. et al. Innate and adaptive T cells in asthmatic patients: relationship to severity and disease mechanisms. *J. Allergy Clin. Immunol.* **136**, 323–333 (2015).
7. Lin, Y. L., Shieh, C. C. & Wang, J. Y. The functional insufficiency of human CD4 +CD25 high T-regulatory cells in allergic asthma is subjected to TNF-α modulation. *Allergy* **63**, 67–74 (2008).
8. Raedler, D. et al. Identification of novel immune phenotypes for allergic and nonallergic childhood asthma. *J. Allergy Clin. Immunol.* **135**, 81–91 (2015).
9. Mamessier, E. et al. T-cell activation during exacerbations: a longitudinal study in refractory asthma. *Allergy* **63**, 1202–1210 (2008).
10. Wegrzyn, A. S. et al. T-cell regulation during viral and nonviral asthma exacerbations. *J. Allergy Clin. Immunol.* **136**, 194–197.e199 (2015).
11. Wang, L. L. et al. Expression of CD39 mRNA is altered in the peripheral blood of patients with allergic asthma. *Biomed. Rep.* **2**, 75–78 (2014).
12. Kusel, M. M. et al. Early-life respiratory viral infections, atopic sensitization, and risk of subsequent development of persistent asthma. *J. Allergy Clin. Immunol.* **119**, 1105–1110 (2007).
13. Sigurs, N. et al. Asthma and allergy patterns over 18 years after severe RSV bronchiolitis in the first year of life. *Thorax* **65**, 1045–1052 (2010).
14. James, K. M. et al. Risk of childhood asthma following infant bronchiolitis during the respiratory syncytial virus season. *J. Allergy Clin. Immunol.* **132**, 227–229 (2013).
15. Holt, P. G. & Sly, P. D. Viral infections and atopy in asthma pathogenesis: new rationales for asthma prevention and treatment. *Nat. Med.* **18**, 726–735 (2012).
16. Oddy, W. H., de Klerk, N. H., Sly, P. D. & Holt, P. G. The effects of respiratory infections, atopy, and breastfeeding on childhood asthma. *Eur. Respir. J.* **19**, 899–905 (2002).
17. Raiden, S. et al. Depletion of circulating regulatory T cells during severe respiratory syncytial virus infection in young children. *Am. J. Respir. Crit. Care Med.* **189**, 865–868 (2014).
18. Christiaansen, A. F. et al. Altered Treg and cytokine responses in RSV-infected infants. *Pediatr. Res.* **80**, 702–709 (2016).
19. Krishnamoorthy, N. et al. Early infection with respiratory syncytial virus impairs regulatory T cell function and increases susceptibility to allergic asthma. *Nat. Med.* **18**, 1525–1530 (2012).
20. Lynch, J. P. et al. Plasmacytoid dendritic cells protect from viral bronchiolitis and asthma through semaphorin 4a—mediated T reg expansion. *J. Exp. Med.* **215**, 537–557 (2018).
21. Lluis, A. et al. Increased regulatory T-cell numbers are associated with farm milk exposure and lower atopic sensitization and asthma in childhood. *J. Allergy Clin. Immunol.* **133**, 551–559 (2014).
22. Schaub, B. et al. Impairment of T-regulatory cells in cord blood of atopic mothers. *J. Allergy Clin. Immunol.* **121**, 1491–1499 (2008).
23. Plantinga, M. et al. Conventional and monocyte-derived CD11b(+) dendritic cells initiate and maintain T helper 2 cell-mediated immunity to house dust mite allergen. *Immunity* **38**, 322–335 (2013).
24. Ullah, M. A. et al. Allergen-induced IL-6 trans-signaling activates gammadelta T cells to promote type 2 and type 17 airway inflammation. *J. Allergy Clin. Immunol.* **136**, 1065–1073 (2015).
25. Huang, Y. et al. IL-25-responsive, lineage-negative KLRG1(hi) cells are multipotential 'inflammatory' type 2 innate lymphoid cells. *Nat. Immunol.* **16**, 161–169 (2015).
26. Masopust, D., Murali-Krishna, K. & Ahmed, R. Quantitating the magnitude of the lymphocytic choriomeningitis virus-specific CD8 T-cell response: it is even bigger than we thought. *J. Virol.* **81**, 2002–2011 (2007).
27. Holgate, S. T. et al. Epithelial-mesenchymal interactions in the pathogenesis of asthma. *J. Allergy Clin. Immunol.* **105**, 193–204 (2000).
28. Byers, D. E. et al. Long-term IL-33–producing epithelial progenitor cells in chronic obstructive lung disease. *J. Clin. Investig.* **123**, 3967–3982 (2013).
29. Ordovas-Montanes, J. et al. Allergic inflammatory memory in human respiratory epithelial progenitor cells. *Nature* **560**, 649–654 (2018).
30. Naik, S. et al. Inflammatory memory sensitizes skin epithelial stem cells to tissue damage. *Nature* **550**, 475–480 (2017).
31. Bendelja, K. et al. Predominant type-2 response in infants with respiratory syncytial virus (RSV) infection demonstrated by cytokine flow cytometry. *Clin. Exp. Immunol.* **121**, 332–338 (2000).
32. Caballero, M. T. et al. TLR4 genotype and environmental LPS mediate RSV bronchiolitis through Th2 polarization. *J. Clin. Investig.* **125**, 571–582 (2015).

33. Kaiko, G. E. et al. Toll-like receptor 7 gene deficiency and early-life Pneumovirus infection interact to predispose toward the development of asthma-like pathology in mice. *J. Allergy Clin. Immunol.* **131**, 1331–1339 (2013).
34. de Heer, H. J. et al. Essential role of lung plasmacytoid dendritic cells in preventing asthmatic reactions to harmless inhaled antigen. *J. Exp. Med.* **200**, 89–98 (2004).
35. Strickland, D. H. et al. Reversal of airway hyperresponsiveness by induction of airway mucosal CD4+CD25+ regulatory T cells. *J. Exp. Med.* **203**, 2649–2660 (2006).
36. van der Veeken, J. et al. Memory of inflammation in regulatory T cells. *Cell* **166**, 977–990 (2016).
37. Sanchez, A. M., Zhu, J., Huang, X. & Yang, Y. The development and function of memory regulatory T cells after acute viral infections. *J. Immunol.* **189**, 2805–2814 (2012).
38. Tubo, N. J. et al. Single naive CD4+ T cells from a diverse repertoire produce different effector cell types during infection. *Cell* **153**, 785–796 (2013).
39. Lloyd, C. M. & Hawrylowicz, C. M. Regulatory T cells in asthma. *Immunity* **31**, 438–449 (2009).
40. Christianson, C. A. et al. Persistence of asthma requires multiple feedback circuits involving type 2 innate lymphoid cells and IL-33. *J. Allergy Clin. Immunol.* **136**, 59–68 (2015).
41. Toussaint, M. et al. Host DNA released by NETosis promotes rhinovirus-induced type-2 allergic asthma exacerbation. *Nat. Med.* **23**, 681–691 (2017).
42. Price, A. E. et al. Systemically dispersed innate IL-13–expressing cells in type 2 immunity. *Proc. Natl Acad. Sci.* **107**, 11489–11494 (2010).
43. Neill, D. R. et al. Nuocytes represent a new innate effector leukocyte that mediates type-2 immunity. *Nature* **464**, 1367–1370 (2010).
44. Lynch, J. P. et al. The plasmacytoid dendritic cell: at the cross-roads in asthma. *Eur. Respir. J.* **43**, 264–275 (2014).
45. Swiecki, M., Gilfillan, S., Vermi, W., Wang, Y. & Colonna, M. Plasmacytoid dendritic cell ablation impacts early interferon responses and antiviral NK and CD8(+) T cell accrual. *Immunity* **33**, 955–966 (2010).
46. Lin, W. et al. Allergic dysregulation and hyperimmunoglobulinemia E in Foxp3 mutant mice. *J. Allergy Clin. Immunol.* **116**, 1106–1115 (2005).
47. Werder, R. B. et al. PGD2/DP2 receptor activation promotes severe viral bronchiolitis by suppressing IFN-lambda production. *Sci. Transl. Med.* **10** eaao0052 (2018).
48. Rock, J. R. et al. Basal cells as stem cells of the mouse trachea and human airway epithelium. *Proc. Natl Acad. Sci.* **106**, 12771–12775 (2009).
49. Phipps, S. et al. Toll/IL-1 signaling is critical for house dust mite-specific helper T cell type 2 and type 17 [corrected] responses. *Am. J. Respir. Crit. Care Med.* **179**, 883–893 (2009).

Figure S1

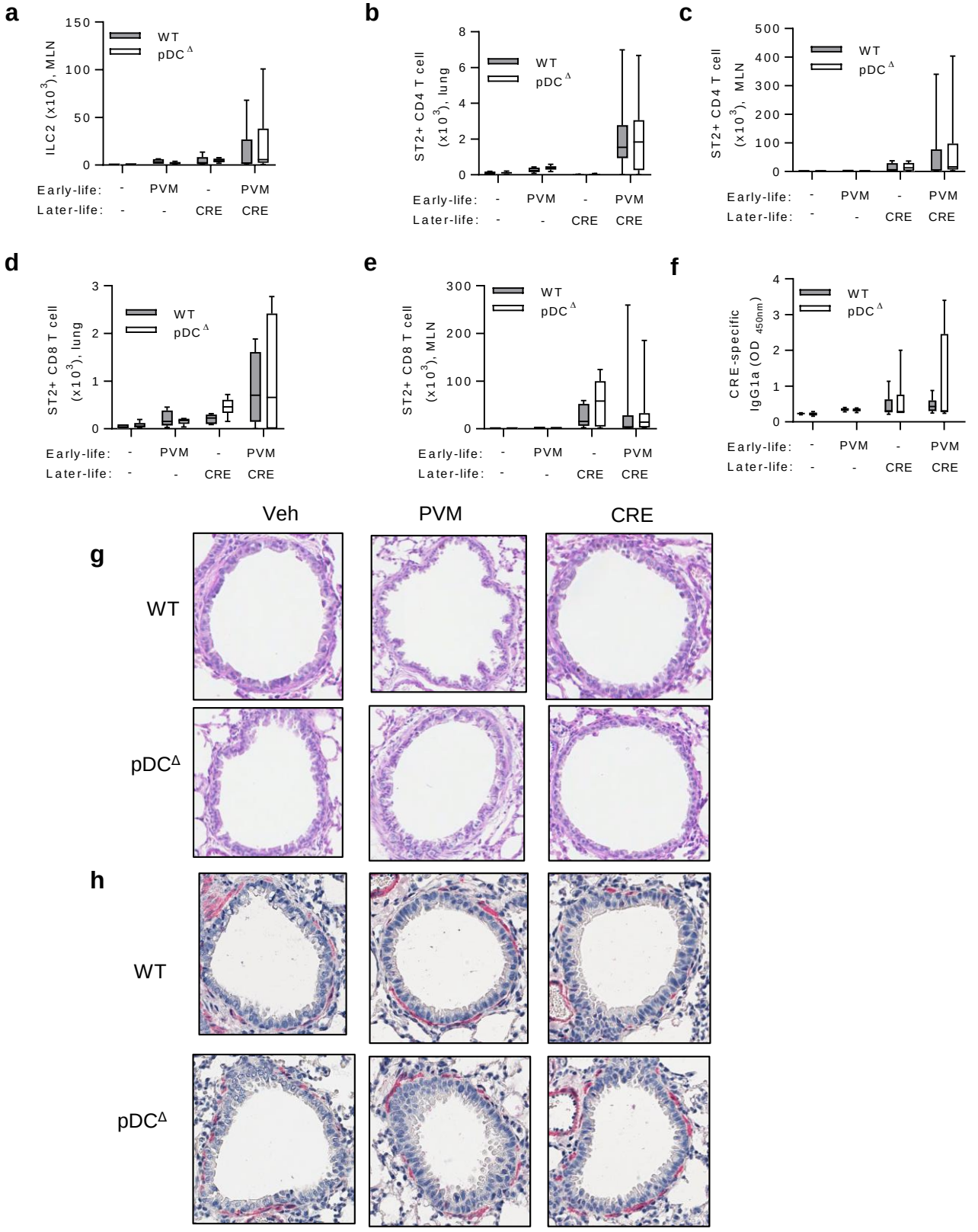

Figure S1

(a) ILC2 (CD2−, CD3−, CD11c−, CD11b−, B220−, Gr-1−, CD25+, ST-2+, and CD90.2+) in MLN. ST2^{hi} CD4+ T cells in lung (b) and MLN (c). ST2^{hi} CD8+ T cells in lung (d) and MLN (e). (f) CRE-specific IgG1a in serum. (g) Mucus producing airway epithelial cells (AECs): representative micrographs (x400 magnification). (h) Airway smooth muscle (ASM) area: representative micrographs (x400 magnification). Data are representative of 6-8 mice per group performed twice and presented as box and whisker plots showing quartiles (boxes) and range (whiskers).

Figure S2

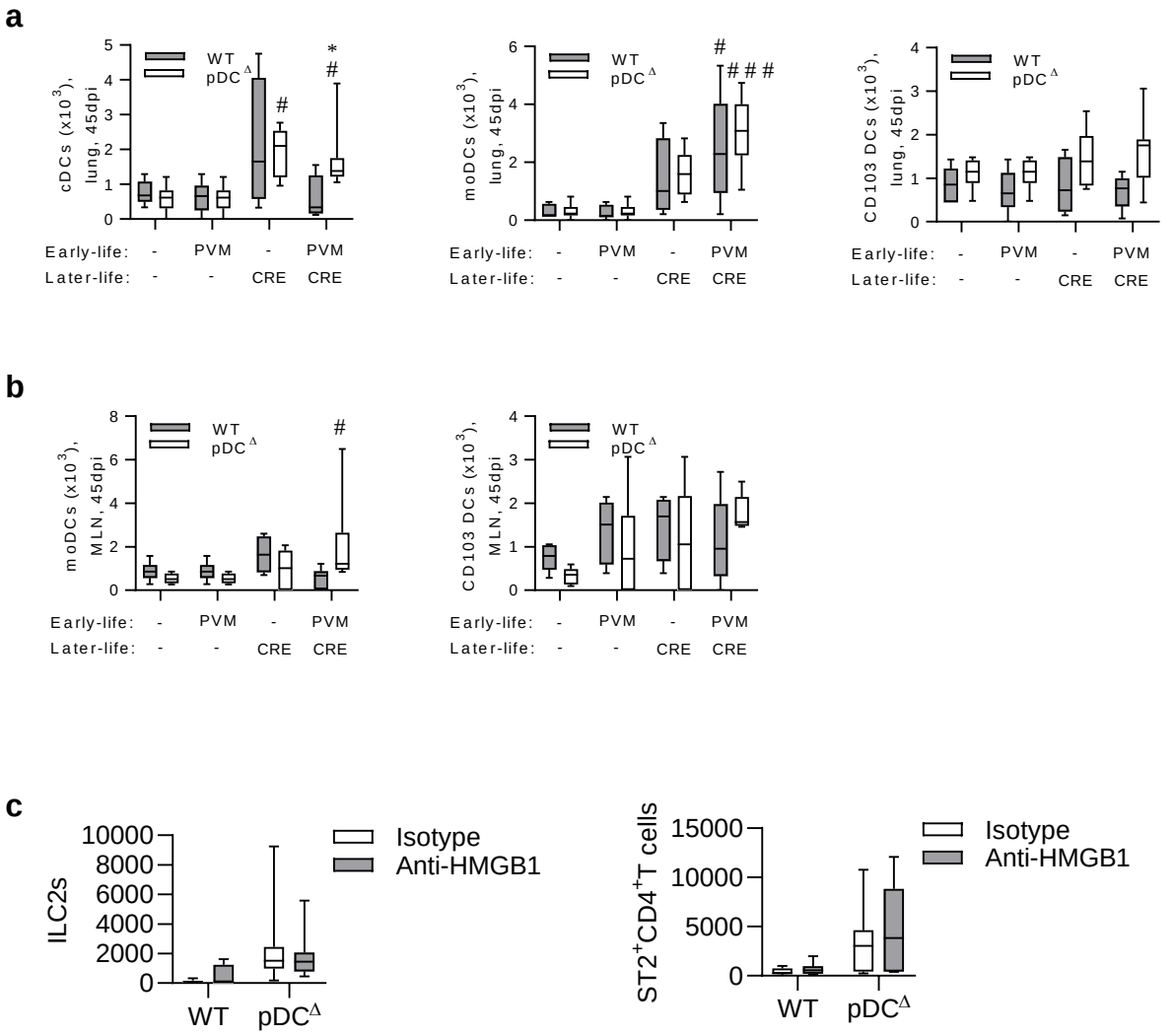

Figure S2

(a) cDCs (F4/80-, CD11c+, CD11b+, MHCII+, CD64-) (left), monocyte-derived (mo)DCs (F4/80-, CD11c+, CD11b+, MHCII+, CD64+) (middle) and CD103 DCs (F4/80-, CD11b-, CD11c+, MHCII+, CD64-, CD103+) (right) in lung. (b) moDCs (left) and CD103 DCs (right) in MLN. (c) ILC2s and ST2+ CD4+ T cells in lung. Data are representative of 6-8 mice per group performed twice and presented as box and whisker plots showing quartiles (boxes) and range (whiskers). *denotes $p<0.05$ and **denotes $p<0.01$ and ***denotes $p<0.001$ compared to WT mice administered PVM and 1x CRE.

Figure S3

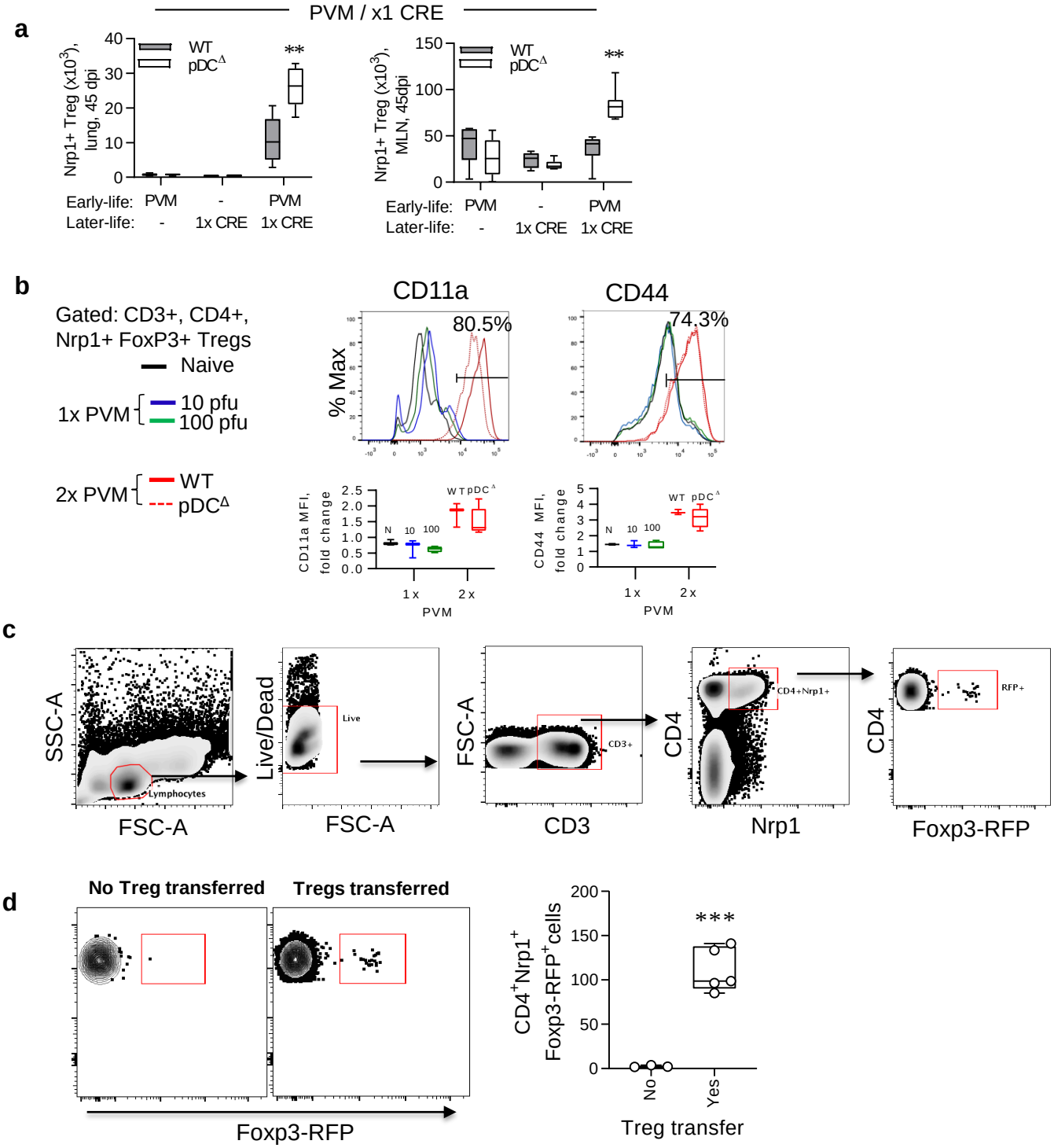

Figure S3

(a) Nrp1+ Treg cells in lung (left) and MLN (right). (b) Representative histogram plots of CD11a and CD44 staining (top panel) and expression of CD11a and CD44 on Nrp1+ Treg cells in MLN. (c) Representative flow cytometry plots of Nrp1+ Treg cell gating. (d) FoxP3-RFP+ Nrp1+ Treg cells in MLN. Data are representative of 4-5 mice per group performed twice and presented whisker plots showing quartiles (boxes) and range (whiskers). *denotes $p<0.05$ and **denotes $p<0.01$ and ***denotes $p<0.001$ compared to WT mice administered PVM and 1x CRE. #denotes $p<0.05$ and ##denotes $p<0.01$ and ###denotes $p<0.001$ compared to veh mice.